IEEE Access
Multidisciplinary | Rapid Review | Open Access Journal

Received 12 May 2023, accepted 5 June 2023, date of publication 9 June 2023, date of current version 15 June 2023.

Digital Object Identifier 10.1109/ACCESS.2023.3284683

RESEARCH ARTICLE

High-Bandwidth Coherent OFDM-Nyquist-TDM Transceiver With Low-Bandwidth Electronics

YOUNUS MANDALAWI, KARANVEER SINGH, (Student Member, IEEE), MOHAMED I. HOSNI, JANOSCH MEIER, AND THOMAS SCHNEIDER

Terahertz-Photonics Group, Technische Universität Braunschweig, 38106 Braunschweig, Germany

Corresponding author: Younus Mandalawi (younus.mandalawi@ihf.tu-bs.de)

This work was supported in part by the Deutsche Forschungsgemeinschaft (DFG, German Research Foundation) under Grant 424608109, Grant 424608271, Grant 424607946, Grant 424608191, Grant 403154102, Grant 403579441, and Grant 322402243.

ABSTRACT We present a broadband coherent orthogonal frequency-division multiplexing (OFDM) transceiver based on orthogonal sampling and low bandwidth electronic analog signal processing. Wideband superchannels, without any guardband are aggregated from low bandwidth OFDM channels in the time domain by orthogonal Nyquist sinc-pulse sequences with a rectangular bandwidth. Therefore, the method is called OFDM-Nyquist-time division multiplexing (TDM). Simulation and experimental results will be discussed for optical systems. However, with some modifications the same principle can be used for wireless or THz signals. In simulations, we show a 40 GHz bandwidth, 160 Gbps, 16-QAM, 128 OFDM x 5-Nyquist-TDM transceiver based on 4 GHz electronics for the digital-to-analog (DAC), analog-to-digital (ADC) conversion and for the digital signal processing, including Fourier transform. For the experiment, we verify the processing of a 24 GHz bandwidth, 48 Gbps QPSK, 512 OFDM x 3-Nyquist-TDM signal with a 4 GHz transmitter and receiver. Since the proposed method drastically decreases the sampling rate and bandwidth requirements for the Fourier processing, the DAC and ADC, it can be a promising alternative for future communication systems with the highest possible symbol rate.

INDEX TERMS Optical frequency comb, Nyquist TDM transmission, optical OFDM, coherent transceiver.

I. INTRODUCTION

With the steady introduction of new applications, technologies, and services, global traffic has been experiencing exponential growth. Over the past decade, the need for high-speed data communication and advanced signal processing has fueled numerous research efforts [1], [2], [3], [4], [5], [6], [7], [8]. Among other multi-carrier modulation techniques, orthogonal frequency division multiplexing (OFDM) has been extensively studied in communication systems as one possibility to meet the exponential rise of internet traffic requirements [1], [2], [3], [4], [5], [6], [7], [8], [9]. OFDM is well known for its many advantages such as subcarrier flexibility, and high spectral efficiency [1], [2], [3], [4], [5], [6], [7], [8], [9]. Wideband OFDM transceivers, however, rely on a high-speed digital-to-analog converter (DAC) in the transmitter and an analog-to-digital converter (ADC) in the receiver [2], [3], [9], [10]. In addition, they require high-speed digital signal processing (DSP) for the Fourier processing in the transmitter and receiver to multiplex and demultiplex the orthogonal subcarriers. High-bandwidth electronics suffer from jitter problems and power consumption. Therefore, several modified OFDM schemes have been proposed as a possible solution [2], [3]. Spectrum slicing, assisted by an optical comb at the receiver has been presented in [2]. However, spectrum slicing has very high demands on the filter functions for sub-band filtering in addition to the increased post-processing complexity for signal reconstruction. A modified low-bandwidth, sub-Nyquist sampling receiving scheme has been proposed for intensity modulation-direct detection (IM-DD) OFDM systems in [3]. The system effectively reduces the bandwidth and sampling rate required for the ADC along with the demands for Fourier processing at the receiver side. This was achieved by an analog demultiplexing of 4 groups of OFDM data subchannels, time multiplexed to a 12.5 GHz bandwidth. However, the digital time multiplexing

The associate editor coordinating the review of this manuscript and approving it for publication was Wei-Wen Hu.

of the subcarriers adds up to the DSP complexity at the transmitter, as it requires digital pre-processing of the data. Additionally, for this method a high sampling rate and bandwidth DAC at the transmitter side is essential. Furthermore, high-bandwidth pulse shaping and digital pre-distortion shaping were required additionally.

In this work, we propose a wideband coherent optical OFDM transceiver concept for optical communications based on orthogonal sampling with sinc-pulse sequences and time-division multiplexing (TDM) in parallel branches as a proof of concept [11], [12]. With some modifications, the same concept might be implemented in various other communication schemes, including radio-over-fiber, free space wireless, Terahertz or millimeter wave communications. The sampling rate and bandwidth of the Fourier processing, as well as that of the DAC and ADC is reduced by the number of branches M [13], [14]. This bandwidth reduction may come with an additional resolution and signal-to-noise and distortion ratio (SINAD) improvement of the received signal. For $M = 3$, for instance, a SINAD improvement of 9 dB is expected [15]. No special pre-processing is required and the orthogonal sampling is achieved by driving an intensity modulator, like an MZM or a ring modulator [16], with sinusoidal radio frequencies, generated by a frequency oscillator (FO). For a frequency down-conversion of the input signal by 3, just one single frequency is required.

The system does not rely on any pulse source or a DAC for pulse generation, DSP, optical filters, nonlinearity, or optical delay lines. Instead, it utilizes single frequency oscillators, electrical phase shifters, multipliers, and properly biased Mach-Zehnder modulators (MZM). Since the bandwidth of the generated superchannel is rectangular, even higher data rate channels can be aggregated by an additional wavelength division multiplexing (WDM). A similar superchannel aggregation without guard band, based on three WDM channels, each of which consisting of three Nyquist TDM sub-channels, was successfully demonstrated for the generation, reception, and processing of high-bandwidth data with low-bandwidth integrated devices [12], [17], [18]. We have presented extensive theoretical studies and background of the system in [12] and especially the accompanied supplementary material. Here, we extend this concept to the widely used OFDM, with greatly reduced DSP bandwidth.

The paper is organized as follows: Section II explains the basic principle of the proposed transceiver. Section III describes the OFDM-Nyquist-TDM-WDM multiplexing. Section IV discusses the simulation. The experimental results are presented in Sec. V. Section VI includes system non-idealities discussion and Sec. VII concludes the paper.

II. BASIC CONCEPT

Before we describe the OFDM-Nyquist-TDM concept, we will first review the idea of orthogonal sampling [11], [19]. Theoretically, a DAC is a Dirac-Delta sequence with the correct repetition rate, weighted with the sampling points and send through a rectangular filter. Due to the rectangular filter shape, any bandwidth-limited signal can be seen as the superposition of single sinc pulses, weighted with the sampling points and time-shifted to each other in a way, that each sampling point of a subsequent sinc pulse is in the zero crossing of the previous. Due to the orthogonality of the sinc pulses, the single sampling point could be retrieved in the receiver by an integration over the multiplication between the incoming signal and a sinc pulse with the right bandwidth and time shift. Dirac-Delta sequences are unlimited in frequency, whereas sinc-pulses are unlimited in time. Thus, both are just mathematical constructs.

Sinc-pulse sequences instead, have the same property of orthogonality, but, are a flat, rectangular, phase-locked frequency comb in the spectral domain [20], [21], [22]. The simplest sinc-pulse sequence (with two zero crossings), is just a single, direct current (DC) shifted sinusoidal frequency, or in the frequency domain, a DC and one single frequency. In the same way as sinc pulses, sinc-pulse sequences can be used to generate and detect each bandwidth-limited signal. The only difference is, that a sinc pulse encodes a single sampling point, whereas a sinc-pulse sequence defines and samples periodic sampling points. For the simplest sinc-pulse sequence (two zero crossings), the repetition time is three times longer than the pulse duration. Therefore, with three identical but time-shifted sinc pulse sequences in three parallel branches, for instance, the whole signal can be generated and received. But, in each branch, the single sinc-pulse sequence, weighted with the periodic sampling points represents a signal with only 1/3rd of the bandwidth and sampling rate. This will be used in the OFDM transceiver. By increasing the number of comb lines, the bandwidth and sampling rate requirements can be further reduced, of course. For M branches, $n = (M\text{-}1)/2$ equidistant RF frequencies from an oscillator are required.

The wideband OFDM-Nyquist-TDM transceiver, consisting of $M = 3$ parallel branches, can be seen in Fig. 1. The wideband OFDM signal has a total bandwidth of B and a total number of orthogonal frequency subcarriers Mx N. In each branch, the I and Q components are generated by a low bandwidth DAC and a conventional OFDM modulation with a $B/(2M)$ bandwidth and N inverse fast Fourier transform (IFFT) points per branch (or the number of orthogonal OFDM channels). Therefore, we have I_0 to I_{M-1} for the Inphase and Q_0 to Q_{M-1}, for the quadrature components, as shown in Fig. 1 for $M = 3$. For the orthogonal multiplexing of the three OFDM signals, we use sinc-pulse sequences with two zero crossings [12]. In the equivalent frequency domain, this corresponds to a flat, three-line frequency comb in the optical domain with a rectangular bandwidth. In the baseband, it is a single, DC-shifted sinusoidal frequency. This frequency is generated by an FO and for each branch time-shifted and weighted with the sampling points of the OFDM sub-channel. The OFDM sub channel weighted sinc-pulse sequences are the blue, red, and yellow traces, shown in Fig.1. The time shift between the sinusoidal frequencies is achieved by a

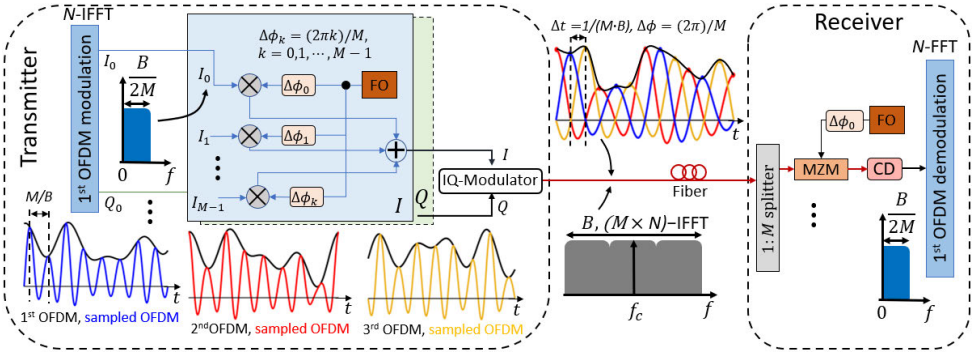

FIGURE 1. Concept figure. The colored lines indicate the different low-bandwidths OFDM sub-signals for M=3. FO: frequency oscillator, MZM: Mach-Zehnder modulator, CD: Coherent detection.

phase change of $\Delta\phi_k = (2\pi k)/M$, where k =0,1, $\cdots$, $M-1$ between the channels. For $M = 3$, this corresponds to 0°, 120°, and 240°. All three phase-shifted and weighted sinusoidals are summed up and used to drive the I or Q branch of an I-Q modulator. The required DC shift of the sinusoidals is accomplished by adjusting the bias of the modulator. A modulator with a bandwidth B_{M} can modulate OFDM signals with the bandwidth $B = 2{\cdot}B_{\mathrm{M}}$. The generated optical signal is transmitted over a standard single-mode fiber (SSMF). Please note that a wireless or THz-OFDM signal can be achieved with the same method. In this case, the sinusoidal together with an additional DC has to be weighted with the sampling points, and the laser and modulator have to be replaced by an appropriate source and mixer.

To demultiplex and receive a low-bandwidth sub-channel from the wideband OFDM-Nyquist-TDM signal, it has to be multiplied with a sinc-pulse sequence with the correct bandwidth and time shift (or phase). For optical signals, this can be done by an intensity modulator driven with a sinusoid with the same frequency as in the transmitter. The required DC shift of the sinusoid is again achieved by adjusting the bias of the modulator. In each of the three branches just 1/3$^{\mathrm{rd}}$ of the sampling points are received, representing again the low bandwidth blue, red, and yellow signals in Fig.1. For the detection of these signals, a coherent detector (CD) with a baseband bandwidth of $B/(2M)$ is sufficient [2] and the bandwidth of the modulator is the same as that in the transmitter $B/2$. The other sub-signals are demultiplexed by driving the modulators in the other branches with the same electrical frequencies but with a phase shift of $\Delta\phi_k$. Finally, the coherently detected $B/(2M)$ low-bandwidth sub OFDM signal is demodulated by a conventional demodulation process with a fast Fourier transform (FFT) of only N.

III. OFDM-NYQUIST-TDM-WDM

In a Nyquist-WDM (N-WDM) system, normal data is shaped to a sinc-shaped Nyquist pulse in the time domain, which corresponds to a rectangular spectrum in the frequency domain [12]. These rectangular individual signals can then be stacked adjacent to each other without a guard band in between in the frequency domain. This enables the transmission at the maximum possible symbol rate. However, in practice, it is impossible to generate an infinitely long sinc-pulse, which is necessary to achieve a perfect rectangular spectrum. As a result, in N-WDM experiments, advanced filtering, spectrum shaping and DSP techniques with high bandwidth have been employed to shape the pulses to resemble a single sinc-pulse as closely as possible [12], [24], [25].

Unlike the Nyquist approach, the faster-than-Nyquist (FTN) technique depends on sending non-orthogonal pulses in the time domain for transmission [26], [27]. In an attempt to improve the spectral efficiency, the time spacing between the pulses (symbol interval) is shortened to pack more data into the same channel. Such a system also requires pulse shaping and the loss of orthogonality results in ISI problems, which must be compensated. This compensation may increase the DSP and hardware detection complexity [26], [27].

OFDM exploits orthogonal sinc-shapes in the frequency domain (please see Fig. 2 (a)). The generation, multiplexing and demultiplexing can be achieved by an inverse or forward Fourier transform of all channels together in a digital signal processor (DSP). However, for high symbol rates, this requires very high bandwidth electronics for the transmitter and receiver [1], [2], [3], [12].

In the proposed OFDM-Nyquist-TDM system, we have combined OFDM (Fig. 2 (a)) with Nyquist TDM (Fig. 2 (b)). In contrast to Nyquist WDM, it is not based on single sinc-pulses, instead, sinc-pulse sequences are used. In the frequency domain, these sinc-pulse sequences are a rectangular frequency comb, which can be produced by a modulator, driven with sinusoidal frequencies [20]. Each individual sequence transmits $1/M$ -times the information of the broadband OFDM signal. Here M is the number of frequencies in the optical comb, or the number of parallel branches in the transmitter and receiver. This should not be confused with the orthogonal OFDM sub-frequencies. In each of the M parts of the OFDM signal, N orthogonal OFDM sub-frequencies with a frequency spacing of Δf_{O} in a total bandwidth of $\Delta f = N\,\Delta f_{\mathrm{O}}$, are used to encode the information with the maximum possible symbol rate. The total bandwidth of the single

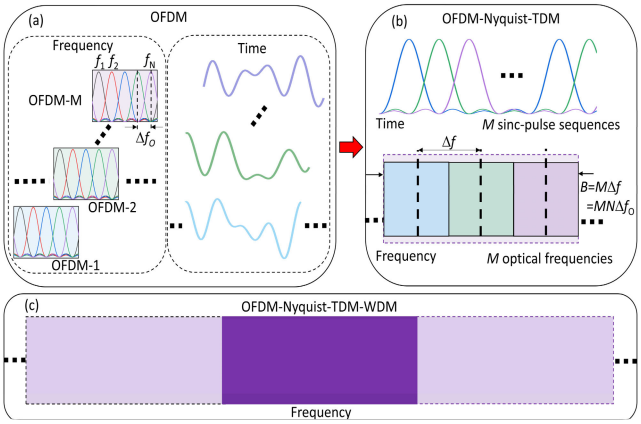

FIGURE 2. OFDM-Nyquist-TDM-WDM multiplexing. N orthogonal OFDM frequencies with the frequency spacing Δf_O are orthogonally multiplexed in the frequency domain to build one of M sub-signals (a). These modulated sub-signals may have a time varying shape, which is orthogonally sampled by one of M sinc-pulse sequences (for instance the blue one in (b)). Then all M sampled signals are orthogonally multiplexed in the time domain to form a rectangular channel with the bandwidth $B = M\Delta f = MN\Delta f_O$ (b). These rectangular channels may be further multiplexed in the frequency domain to build an OFDM-Nyquist-TDM-WDM superchannel without any guard band (c).

OFDM sub-signal Δf coincides with the frequency spacing between the comb lines. Therefore, these OFDM frequencies are orthogonal in the frequency domain. Additionally, all the M sinc-pulse sequences are orthogonal in the time domain. Thus, the orthogonal frequency domain sub channels can additionally be multiplexed in the time domain. Due to orthogonality, this multiplexing can as well be carried out with the maximum possible symbol rate. So, the broadband OFDM-Nyquist-TDM signal consists of M x N OFDM sub frequencies with a total bandwidth of $B = M\Delta f = MN\Delta f_O$ But, for the generation, detection and processing of the signal with the aggregated bandwidth B, ADC, DAC and DSP with a bandwidth of $\Delta f/2 = B/(2M)$ are sufficient. Moreover, the OFDM-Nyquist-TDM signal has a rectangular bandwidth. Therefore, as for Nyquist-WDM, the OFDM-Nyquist-TDM channels can be further aggregated without any guard band to OFDM-Nyquist-TDM-WDM superchannels (Fig. 2 (c)). For the generation and detection of these superchannels again only electronics with a bandwidth of $B/(2M)$ would be necessary [12].

IV. SIMULATION SETUP AND RESULTS

This section describes the simulation setup and achieved results for the proposed OFDM-Nyquist-TDM transceiver system, obtained by the Optisystem software.

A. SIMULATION SETUP

Figure 3 illustrates a schematic diagram for the simulation of the OFDM-Nyquist-TDM transceiver. In the transmitter, three 8 GBd OFDM sub-channels (M = 3) were generated with a baseband width of 4 GHz (B/2M) for the I and Q components to build a 24 GHz optical bandwidth OFDM-Nyquist-TDM signal with 24 GBd symbol rate.

For each sub-channel, the I and Q components are generated by mapping a stream of pseudo-random bit sequence (PRBS) data with 16-, 32- and 64-quadrature amplitude modulation (QAM) formats. The signal is then feet to an N-IFFT with $N = 128$ subcarriers. All frequency subcarriers were used for data transmission except for the middle one, which is preserved for the suppressed optical carrier. After that, a 5% cyclic prefix (CP) is assigned to reduce the effect of inter-symbol interference and the parallel signal is converted to a serial data stream.

In each of the three branches, the digital data is converted by a 4 GHz DAC to an analog I and Q waveform. After that, all 3 sub-channels ($\boldsymbol{I_0}$,$\boldsymbol{I_1}$ and $\boldsymbol{I_2}$, and $\boldsymbol{Q_0}$,$\boldsymbol{Q_1}$ and $\boldsymbol{Q_2}$) are multiplied, or orthogonally sampled with three, phase-shifted 8 GHz radio frequencies from an FO. These sub-channels are then orthogonally added up by an analog adder. The superposed 24 GBd I and Q components are modulated to an optical wave in the conventional band of optical telecommunications (193,1 THz) through a 12 GHz bandwidth IQ-modulator, which is properly biased to generate a multiplexed signal of $B = 24$ GHz total bandwidth (3×128 OFDM sub-channels). The corresponding total transmitted netto data rate is 96, 120, and 144 Gbps with 16-, 32-, and 64-QAM, respectively.

The output signal from the IQ-Modulator is amplified via an Erbium-doped fiber amplifier (EDFA) to compensate for the power loss and filtered with a 1 nm optical bandpass filter to reduce the amplified spontaneous emission (ASE) noise. The signal is then sent through an SSMF of 5 km length with a 16 ps/(nm·km) dispersion coefficient. For the presented simulations, all noise parameters (e.g., shot noise, thermal noise, noise figure, ASE noise) for all the components of the setup were turned on. The CW laser has 100 kHz linewidth. The EDFA was assumed to have a noise figure of 4 dB and for the dark current of the balanced photodiodes 5 nA were assumed.

At the receiver, the 24 GHz signal is first split into three branches by a power splitter. In each branch, the signal is multiplied with a phase-shifted sinc-pulse sequence of M/B repetition rate by an MZM to demultiplex the three sub-signals. The MZMs in the 1st, 2nd, and 3rd branches are driven with the same 8 GHz radio frequency and 0°, 120°, and 240° phase shifts to recover the 1st, 2nd, and 3rd OFDM sub-signals, respectively. The demultiplexed signal is then detected in parallel with a coherent detector (CD) of 4 GHz bandwidth. Finally, in each branch the 4 GHz OFDM sub-signal is demodulated using the inverse of the modulation process.

A 5 sub-channel ($M = 5$) system was also simulated by orthogonally superimposing 5 analog 4 GHz OFDM sub-signals. For this, the signal has to be multiplied with a sinc pulse sequence with four zero crossings. This can be achieved by driving the modulator in the transmitter and receiver with radio frequencies of 8 and 16 GHz. These two frequencies are used for all 5 branches but with a $360°/5 = 72°$ phase shift in between. The five channels are then added up and transferred

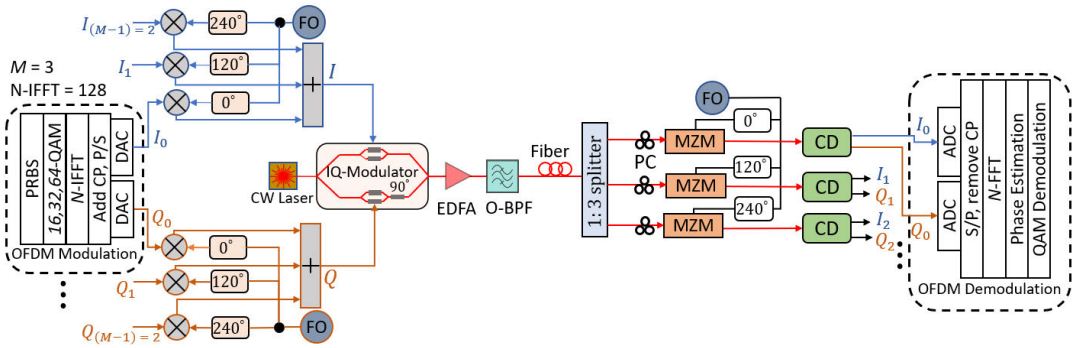

FIGURE 3. Simulation setup for the proposed system. CW: Continuous wave laser, EDFA: Erbium-doped fiber amplifier, O-BPF: Optical band pass filter, PC: Polarization controller. For 5-channels a 1-to-5 splitter and two additional branches with a phase shift of $k \times 72°$, with $k = 0,..,5$ are needed.

to the optical domain by a 20 GHz IQ-modulator. The total symbol rate of the multiplexed superchannel is 40 GBd (40 GHz bandwidth and 160 Gbps with 16-QAM mapping of the 5 × 128 OFDM sub-channels).

In the receiver, the signal is split into 5 branches, multiplied with a sinc-pulse sequence with 4 zero crossings in the modulator and detected and processed with a 4 GHz bandwidth CD and DSP.

B. SIMULATION RESULTS

The optical spectrum of the generated 24 Gbd, 16-QAM OFDM-Nyquist-TDM signal is depicted in Fig. 4 (a). Since we are using OFDM and Nyquist-TDM together, the rectangular bandwidth signal contains the maximum possible symbol rate. In the receiver, the OFDM signal is demultiplexed by multiplying it with a sinc-pulse sequence with two zero crossings. In the equivalent frequency domain, this is the convolution between the rectangular OFDM spectrum and a rectangular, three-line frequency comb with the same bandwidth. The result is the triangular spectrum, which can be seen in Fig. 4 (b). Only the central 8 GHz optical bandwidth part is detected by the 4 GHz baseband bandwidth CD.

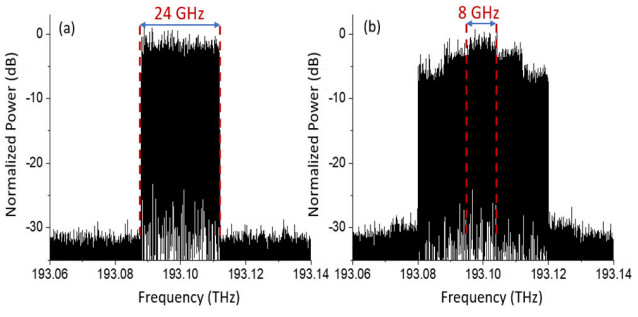

FIGURE 4. Optical spectrum of the 3-channel, 16-QAM OFDM-Nyquist-TDM (24 GHz total bandwidth) signal (a), and (b), for the demultiplexed single channel after the modulator in the receiver. Please note, that the baseband width of the 8 GHz in the middle correspond to 4 GHz, which are detected by the CD and processed by the DSP.

Figure 5 shows the calculated Q-Factor in dependence on the optical signal-to-noise ratio (OSNR) for the signal. The Q-Factor values, which were calculated from the

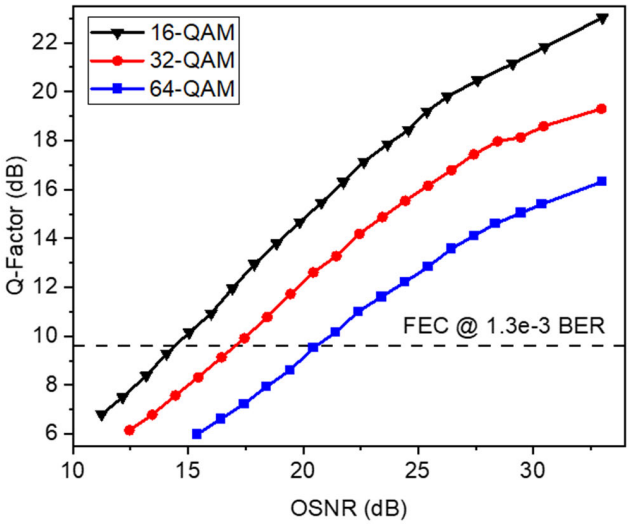

FIGURE 5. OSNR versus Q-Factor for the 3-sub channel, 24 GHz OFDM-Nyquist-TDM signal with 16-,32-, and 64-QAM in a back-to-back (B2B) configuration.

constellation mean (μ) and standard deviation (σ) values [1], [28], are shown for 16-, 32-, and 64-QAM OFDM signals for a back-to-back (B2B) configuration. The threshold at which the signal can still be transmitted error free by adding an additional forward error correction (FEC) [29] is presented by the dashed line. As can be seen, OSNRs of around 14.4, 17.1, and 20.5 dB are required to reach the 9.6 dB Q-Factor threshold for 16-, 32-, and 64-QAM, respectively.

Fig. 6 shows the bit error rate (BER) against the OSNR for the same system. The BER was calculated from the error vector magnitude (EVM) as described in [30]. At the 1.3E-3 BER threshold, an EVM% of 15.3, 10.8, and 7.7 were obtained for an OSNR of around 14.4, 17.1, and 20.5 dB, with 16-, 32-, and 64-QAM, respectively.

The constellation diagrams of the recovered three channels at the receiver for a back-to-back (B2B) configuration are shown in Fig. 7 (a), (b), and (c). The calculated average EVM% for the 22.3 dB Q-factor is 3.43 with zero bit errors, proving the successful demultiplexing by the proposed method. The constellation diagrams after 5 km SSMF are shown in Fig. 7 (d), (e), and (f). For the 16 dB Q-factor

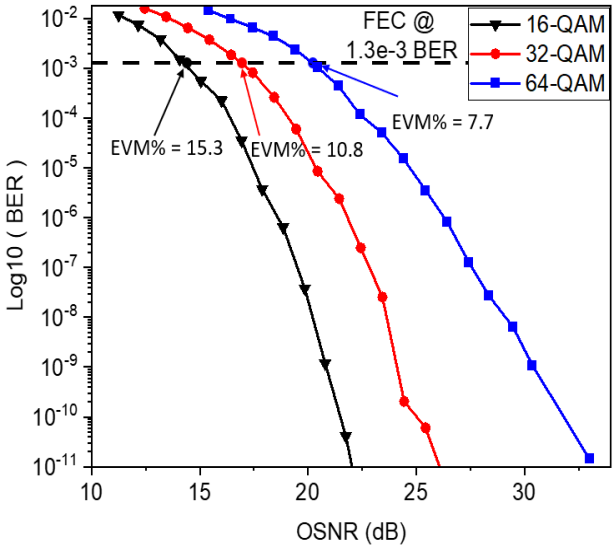

FIGURE 6. Calculated Log10 (BER) as a function of OSNR for the 24 GHz OFDM-Nyquist-TDM signal with 16-,32-, and 64-QAM.

the demultiplexed sub-channels have 7.14 EVM% on average with a BER of 1.4E-10. It should be noted, that we did not implement any nonlinearity or chromatic dispersion compensation.

The constellation diagrams of the recovered three channels at the receiver for a back-to-back (B2B) configuration are shown in Fig. 7 (a), (b), and (c). The calculated average EVM% for the 22.3 dB Q-factor is 3.43 with zero bit errors, proving the successful demultiplexing by the proposed method. The constellation diagrams after 5 km SSMF are shown in Fig. 7 (d), (e), and (f). For the 16 dB Q-factor the demultiplexed sub-channels have 7.14 EVM% on average with a BER of 1.4E-10. It should be noted, that we did not implement any nonlinearity or chromatic dispersion compensation.

To show the expandability and flexibility of the proposed transceiver, 5-channels with a total bandwidth of 40 GHz and a data rate of 160 Gbps (16-QAM) were simulated. The optical spectrum of the transmitted an demultiplexed signal is depicted in Fig. 8 (a) and (b). Only the 4 GHz part of the demultiplexed spectrum will be detected and processed. Furthermore, the Fourier processing power is reduced by 5, from 20 to 4 GHz.

The constellation diagrams for the 1st, 3rd, and 5th sub-channel are shown in Fig 9 for the B2B case (left) and 5 km transmission in an SSMF (right). The average EVM% for the B2B case was 3.42 without errors and a Q-Factor of 22.32 dB. After a 5 km SSMF transmission, the EVM% was 11.31, resulting in a BER of 2.8E-5 and 12 dB Q-factor.

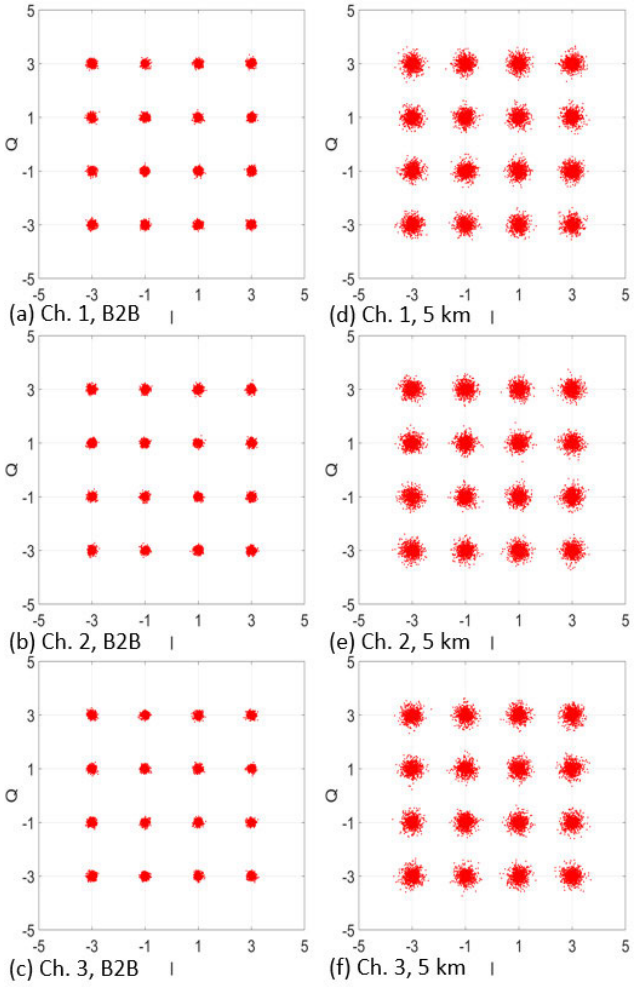

FIGURE 7. Received constellation diagrams of the 3 sub-channel, 24 GHz OFDM-Nyquist-TDM, 16-QAM, signal for B2B, (a), (b), and (c)), and 5 km of SSMF ((d), (e), and (f)).

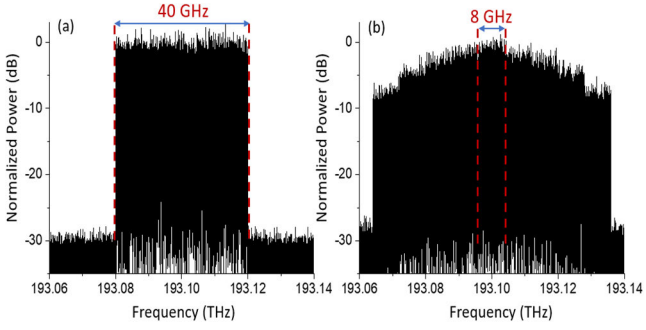

FIGURE 8. Optical 40 GHz spectrum for the 5-channel, 16-QAM OFDM (a), and (b) for the demultiplexing after the modulator in a single branch of the receiver. Please note that here again only the 8 GHz in the middle are detected by the 4 GHz CD.

V. EXPERIMENTAL SETUP AND RESULTS

A. EXPERIMENTAL SETUP

To validate the proposed OFDM-Nyquist-TDM transceiver, proof of concept experiments were carried out. The setup is shown in Fig. 10. For the sake of simplicity and due to a lack of equipment, only one arbitrary waveform generator (AWG) was used in the transmitter for I and another one for Q. The 48 Gbps OFDM signals were generated and multiplexed

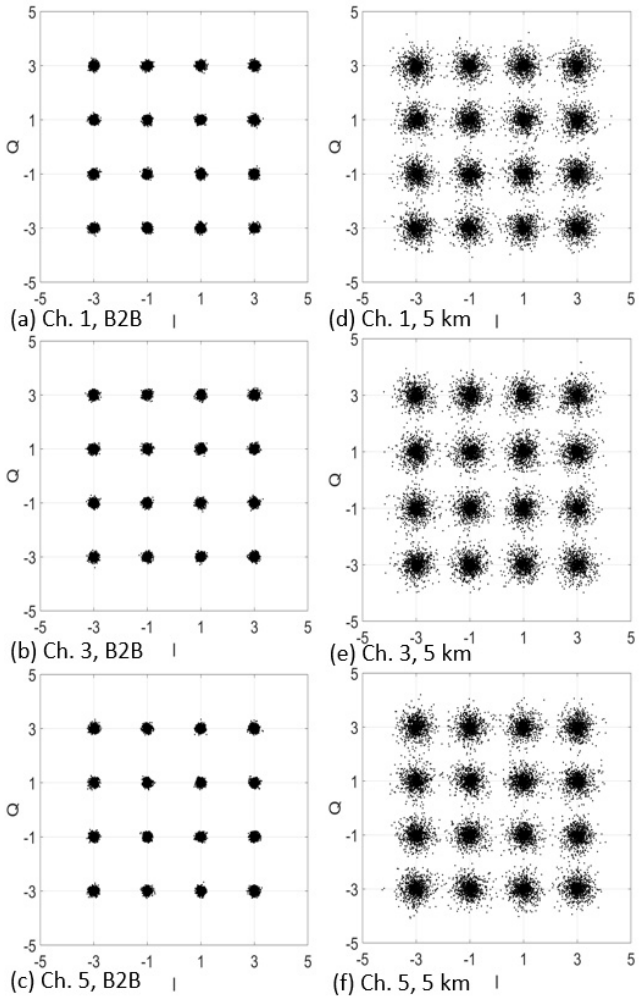

FIGURE 9. Received constellation diagrams of the 1st (top), 3rd (middle), and 5th (bottom) channel from the 5-channel, 40 GHz OFDM-Nyquist-TDM signal (4 GHz baseband bandwidth each) with 16-QAM for (a), (b), and (c) B2B, and (d), (e), and (f) 5 km of SSMF.

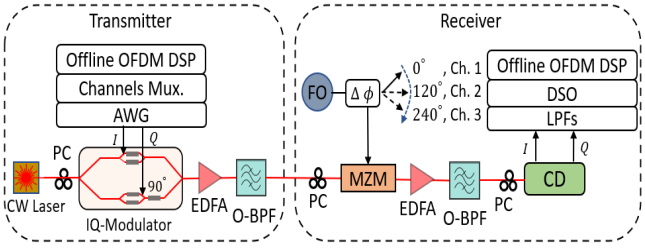

FIGURE 10. Experimental setup for a 3-channel OFDM-Nyquist-TDM transceiver. AWG: arbitrary waveform generator, DSO: digital storage oscilloscope.

by the described method, but offline with MATLAB. The sampling rate and bandwidth of the DAC has restricted the maximum possible data rate to 48 Gbps. The demultiplexing was done subsequently in a single branch by an appropriate phase shift adjustment of the sinusoidal signal. Since a PRBS was used, which is periodic anyway, the broadband signal has been calculated from the sub-signals by offline post-processing.

As optical source, a fiber laser (NKT photonics ADJUSTIK E15) at 1550.116 nm was implemented. Each of the $M = 3$ sub-channels contains $N = 512$ OFDM subcarriers with 4-QAM, modulated with a PRBS. All the subcarriers except the middle one, which was left for the suppressed optical carrier, were carrying data and a CP of 5% was added. The generation of the OFDM signal follows the ordinary process as described in Section III. A without additional DSP or pre-distortion. The three sub-channels were summed up after being multiplied with a single tone, 8 GHz sinusoidal signal with a proper bias and phase shift of 0°, 120°, and 240°, respectively. The components were then uploaded into an AWG (AWG7001A) for I and another one for Q working at a sampling rate of 48 GSs. Therefore, each OFDM has an optical bandwidth of 8 GHz (4 GHz baseband for I and Q). The outputs of the AWGs were fed to an IQ-modulator which was biased properly to achieve a linear modulation. An EDFA together with a 1 nm bandpass filter, for reducing the ASE noise, were used to amplify the signal.

To demultiplex the 8 GHz OFDM sub-channel from the 24 GHz superchannel, the incoming signal was fed to a single, properly biased MZM, driven with an 8 GHz frequency with a certain phase shift. The demultiplexed signal was detected by a CD (OM 3245). Since the CD had a higher bandwidth than the required 4 GHz, we have used digital lowpass filtering after detection. Finally, the signal was recorded with a real-time oscilloscope (Tektronix DPO73304) and the OFDM demodulation and analyses were carried out offline with MATLAB.

B. EXPERIMENTAL RESULTS

The optical spectrum of the 512 × 3, 4-QAM OFDM-Nyquist-TDM superchannel is plotted in Fig. 11 (a) and the demultiplexed 8 GHz single sub-channel spectrum after the MZM in the receiver can be seen in Fig. 11 (b).

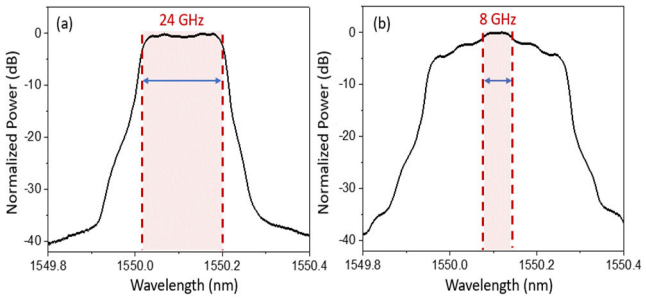

FIGURE 11. Optical spectrum of the transmitted 512 × 3, 4-QAM OFDM signal (a), and (b) for the demultiplexed signal after the modulator in the receiver (8 GHz bandwidth). Please note that the deviation from the rectangular shape is mainly due to the limited spectral resolution of the OSA.

Figure 12 presents the measured constellation and eye diagrams of the successfully recovered and demodulated three

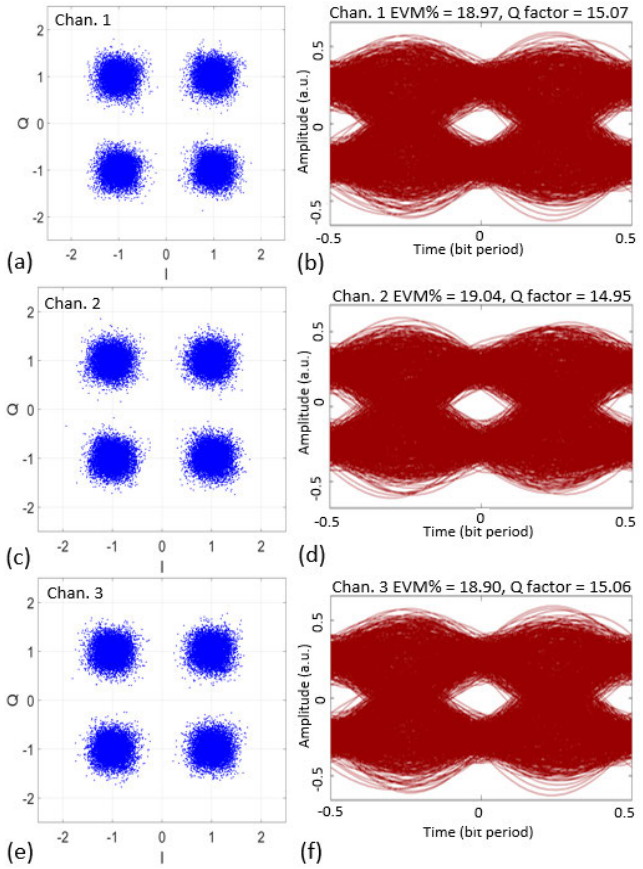

FIGURE 12. Constellation and eye diagrams for the 1st (a, b), 2nd (c, d), and third channel (e, f) for the B2B case.

sub-channels. The average measured EVM% was 18.97 and the BER was 6.76E-8 with clean constellation diagrams and a clear eye-opening.

VI. DISCUSSION

The orthogonality of the TDM multiplexing depends on the time shift between the single sinc-pulse sequences. In the proposed method, this time shift can be precisely controlled by the electrical phase of the sinusoidal signals. At the receiver, the phase shifter can be scanned and locked to the maximum eye-opening of the recovered data [12], for instance. Nevertheless, a moderate change of the phase does not severely degrade the transmission as shown in [12]. To observe the penalty for the Q-Factor and EVM when changing the ideal time shift (phase shift) at the receiver, a simulation verification has been done for a 24 Gbd, 16-QAM, three sub-channel OFDM system. Almost no performance penalty was noticeable for a time inaccuracy of up to 200 fs. Even for a relatively high time inaccuracy of 1 ps, which corresponds to a phase change of 0.8 % (2.88°) for the 8 GHz RF signal, the Q-Factor showed a penalty of 4 dB and the EVM penalty was 2%, compared to the ideal case. Phase shifters with a phase accuracy of ±0.35° for an 8 GHz frequency are available on the market [31]. In a 65 nm CMOS platform, a phase shifter from 21 GHz to 30 GHz with a phase error from 0.28° to 0.88° has been shown [32]. Even for higher frequencies (56 GHz to 65 GHz), a phase error of 1.4° was reported in [33].

Reducing the input frequency and bandwidth of the DAC and ADC is accompanied with a signal quality improvement in terms of achievable signal-to-noise and distortion (SINAD) ratio and with a resolution improvement (effective number of bit (ENOB)). We have investigated this improvement for orthogonal sampling-assisted ADC [15]. The SINAD of an ADC increases quadratically with the jitter. Although even integrated oscillators can show jitter values of 20 fs, state-of-the-art electronic ADC have jitter values of around 100 fs [23]. This is because even for very low jitter clock sources an electronic ADC shows an additional aperture jitter, which means that; even for very stable clock signals, the actual switching time of the sample and hold stage in an electronic ADC is uncertain. This is not the case for orthogonal sampling-assisted ADC. For a 10 fs jitter of the orthogonal sampling and a 100 fs jitter of the following electronic ADC, the SINAD can be improved by 9 dB for 3 branches, higher improvements are possible by increasing the number of branches [15].

The effect of non-idealities on the sinc-shaped Nyquist pulse generation has been studied in detail for different roll-of-factor, ripple and sideband suppression ratios [34], [35]. Compared to an ideal flat comb, a 2 dB ripple in a 3-line comb only increases the root mean square error of the pulses by 3%. This value is decreased for a higher number of comb lines (1.9 % for a 5-line comb). In a recent work, we have investigated the effect of non-ideal combs on the signal-to-noise and distortion (SINAD) ratio achievable in orthogonal sampling assisted analog-to-digital converters [15]. For a three-line comb with a 3 dB ripple the SINAD penalty was around 2 and for a nine-line comb 1 dB [15]. However, even for an integrated, monolithic, electronic-photonic modulator chip (ePIC-MZM), the measured ripple of a three-line comb was less than 0.1 dB [35]. Additionally, the flatness of the comb can be locked to the eye-opening of the received data and adjusted by the biasing point of the MZM modulator, for instance.

Since the scheme utilizes frequency (OFDM) and time (Nyquist TDM) multiplexing techniques, we believe that it is sensitive to fiber dispersion at long distances. This can be compensated by electronic pre- or post-dispersion compensation techniques, or by dispersion compensating fibers. However, the implementation of these methods may require further investigation. For a single carrier Nyquist-TDM, the transmission of 4-QAM, 24 GBd over 40 km of fiber with a Q-factor of 14.48 dB has been shown [12] without any pre- or post-processing of the data. By a digital dispersion compensation, Nyquist-TDM-WDM 112.5 Gbd DP-QPSK data has been transmitted over 640 km of fiber [36]. Additionally, a Nyquist pulse TDM transmission over 525 km with 160 GBd was also demonstrated with a dispersion-managed fiber link [37]. E

VII. CONCLUSION

In conclusion, we have presented by simulation and in a proof-of-concept experiment a wideband coherent optical OFDM-Nyquist-TDM transceiver system that dramatically reduces the necessary electronic bandwidth for the DAC, ADC, and Fourier transform in the transmitter and receiver. Especially the bandwidth reduction of the processed signal is accompanied with a higher resolution of the electronic DAC and ADC and may therefore offer an improved signal-to-noise and distortion ratio for the received signal [15]. This is achieved by orthogonal multiplexing of M-OFDM sub-channels in the time domain by Nyquist sinc-pulse sequences. The transmitter only uses an IQ-modulator, and electrical components like a frequency oscillator, phase shifters, mixers, and an adder. The OFDM sub-signals are demultiplexed and received in M parallel branches by a single MZM and low bandwidth CD, ADC, and electronic signal processing. In simulations, a 5-channel OFDM-Nyquist-TDM with a total data rate of 160 Gbps was detected and processed by 4 GHz electronics. The signal was transmitted over 5 km of SSMF with a BER of 2.8E-5 without using any pre- or post-compensation. Moreover, an experimental proof-of-concept for a 3-channel system with a 24 GHz signal bandwidth, requiring 4 GHz electronics was demonstrated. Due to the reduced bandwidth for the DAC, ADC, Fourier processing, and DSP, the presented method could be a potential solution to keep up with continuously increasing data rates in future communication systems.

REFERENCES

[1] A. J. Lowery, L. B. Du, and J. Armstrong, "Performance of optical OFDM in ultralong-haul WDM lightwave systems," *J. Lightw. Technol.*, vol. 25, no. 1, pp. 131–138, Jan. 2007, doi: 10.1109/JLT.2006.888161.

[2] H. Hu, V. Ataie, E. Myslivets, and S. Radic, "Optical comb assisted OFDM RF receiver," *J. Lightw. Technol.*, vol. 37, no. 4, pp. 1280–1287, Feb. 15, 2019, doi: 10.1109/JLT.2019.2892147.

[3] Z. Luo, F. Li, W. Ni, L. Rong, W. Wang, M. Yin, Q. Sui, and Z. Li, "Modified low-bandwidth sub-Nyquist sampling receiving scheme in an IM/DD OFDM system enabled by improved optical shaping," *Opt. Exp.*, vol. 30, no. 18, 2022, Art. no. 32731, doi: 10.1364/oe.462705.

[4] Y. N. A. Mandalawi, S. Yaakob, W. A. W. Adnan, M. H. Yaacob, and Z. Zan, "Laser phase noise effect and reduction in self-homodyne optical OFDM transmission system," *Opt. Lett.*, vol. 44, no. 2, p. 307, Jan. 2019, doi: 10.1364/OL.44.000307.

[5] Y. N. Ali Mandalawi, S. Yaakob, W. A. W. Adnan, R. S. A. R. Abdullah, M. H. Yaacob, and Z. Zan, "Reduction of phase-modulation to intensity-modulation conversion noise effect using delayed self-homodyne optical orthogonal frequency division multiplexing system," *IEEE Photon. J.*, vol. 13, no. 1, pp. 1–17, Feb. 2021, doi: 10.1109/JPHOT.2020.3045095.

[6] R. Bai and S. Hranilovic, "Kramers–Kronig optical OFDM for bandlimited intensity modulated visible light communications," *J. Lightw. Technol.*, vol. 39, no. 22, pp. 7135–7145, Nov. 15, 2021, doi: 10.1109/JLT.2021.3110661.

[7] A. Güner, "Coherent optical OFDM with index modulation for long-haul transmission in optical communication systems," *IEEE Access*, vol. 10, pp. 46504–46512, 2022, doi: 10.1109/ACCESS.2022.3171050.

[8] L. N. Venkatasubramani, "Demonstration of 608 gbps CO-OFDM transmission using gain switched comb," in *Proc. Conf. Lasers Electro-Opt.*, Washington, DC, USA: Optica Publishing Group, 2020, pp. 1–2, doi: 10.1364/CLEO_AT.2020.JTu2E.9.

[9] O. Lang, R. Feger, C. Hofbauer, and M. Huemer, "OFDM radar with subcarrier aliasing—Reducing the ADC sampling frequency without losing range resolution," *IEEE Trans. Veh. Technol.*, vol. 71, no. 10, pp. 10241–10253, Oct. 2022, doi: 10.1109/TVT.2022.3188511.

[10] S. Varughese, D. Lippiatt, S. Tibuleac, and S. E. Ralph, "Frequency dependent ENoB requirements for 400G/600G/800G optical links," *J. Lightw. Technol.*, vol. 38, no. 18, pp. 5008–5016, Sep. 15, 2020, doi: 10.1109/JLT.2020.3000177.

[11] S. Preußler, G. R. Mehrpoor, and T. Schneider, "Frequency-time coherence for all-optical sampling without optical pulse source," *Sci. Rep.*, vol. 6, no. 1, pp. 1–10, Sep. 2016, doi: 10.1038/srep34500.

[12] A. Misra, J. Meier, S. Preussler, K. Singh, and T. Schneider, "Agnostic sampling transceiver," *Opt. Exp.*, vol. 29, no. 10, p. 14828, 2021, doi: 10.1364/oe.425548.

[13] K. Singh, J. Meier, A. Misra, S. Preubler, J. C. Scheytt, and T. Schneider, "Photonic arbitrary waveform generation with three times the sampling rate of the modulator bandwidth," *IEEE Photon. Technol. Lett.*, vol. 32, no. 24, pp. 1544–1547, Dec. 15, 2020, doi: 10.1109/LPT.2020.3039621.

[14] Y. Mandalawi, "High-bandwidth signal reception with improved ENOB by frequency-time coherence photonics sampling," in *Proc. Optica Adv. Photon. Congr.*, 2022, doi: 10.1364/sppcom.2022.sptu4j.4.

[15] Y. Mandalawi, J. Meier, K. Singh, M. I. Hosni, S. De, and T. Schneider, "Analysis of bandwidth reduction and resolution improvement for photonics-assisted ADC," *J. Lightw. Technol.*, early access, May 25, 2023, doi: 10.1109/JLT.2023.3279876.

[16] M. I. Hosni, K. Singh, S. Dev, A. Zarif, S. Preussler, A. M. Mokhtar, K. Jamshidi, and T. Schneider, "Low power, compact integrated photonic sampler based on a silicon ring modulator," *IEEE Photon. J.*, vol. 14, no. 4, pp. 1–6, Aug. 2022, doi: 10.1109/JPHOT.2022.3197300.

[17] A. Misra, C. Kress, K. Singh, J. Meier, T. Schwabe, S. Preussler, J. C. Scheytt, and T. Schneider, "Reconfigurable and real-time high-bandwidth Nyquist signal detection with low-bandwidth in silicon photonics," *Opt. Exp.*, vol. 30, no. 8, p. 13776, 2022, doi: 10.1364/oe.454163.

[18] M. I. Hosni, K. Singh, Y. Mandalawi, J. Meier, A. M. Mokhtar, and T. Schneider, "Filterless and compact ANy-WDM transmission system based on cascaded ring modulators," *IEEE Access*, vol. 10, pp. 122226–122233, 2022, doi: 10.1109/ACCESS.2022.3222316.

[19] J. Meier, A. Misra, S. Preußler, and T. Schneider, "Orthogonal full-field optical sampling," *IEEE Photon. J.*, vol. 11, no. 2, pp. 1–9, Apr. 2019, doi: 10.1109/JPHOT.2019.2902726.

[20] M. A. Soto, M. Alem, M. A. Shoaie, A. Vedadi, C.-S. Brès, L. Thévenaz, and T. Schneider, "Optical sinc-shaped Nyquist pulses of exceptional quality," *Nature Commun.*, vol. 4, no. 1, pp. 1–11, Dec. 2013, doi: 10.1038/ncomms3898.

[21] S. Preussler, N. Wenzel, and T. Schneider, "Flat, rectangular frequency comb generation with tunable bandwidth and frequency spacing," *Opt. Lett.*, vol. 39, no. 6, p. 1637, Mar. 2014, doi: 10.1364/OL.39.001637.

[22] K. Singh, J. Meier, C. Kress, A. Misra, T. Schwabe, S. Preußler, J. Christoph Scheytt, and T. Schneider, "Emulation of integrated high-bandwidth photonic AWG using low-speed electronics," *Proc. SPIE*, vol. 12028, pp. 42–48, Mar. 2022, doi: 10.1117/12.2609416.

[23] S. Levantino, "Recent advances in high-performance frequency synthesizer design," in *Proc. IEEE Custom Integr. Circuits Conf. (CICC)*, Apr. 2022, pp. 1–7, doi: 10.1109/CICC53496.2022.9772842.

[24] R. Schmogrow, S. Ben-Ezra, P. C. Schindler, B. Nebendahl, C. Koos, W. Freude, and J. Leuthold, "Pulse-shaping with digital, electrical, and optical filters—A comparison," *J. Lightw. Technol.*, vol. 31, no. 15, pp. 2570–2577, Aug. 2013, doi: 10.1109/JLT.2013.2271513.

[25] M. Nakazawa, M. Yoshida, and T. Hirooka, "The Nyquist laser," *Optica*, vol. 1, no. 1, p. 15, 2014, doi: 10.1364/optica.1.000015.

[26] T. Ishihara, S. Sugiura, and L. Hanzo, "The evolution of Faster-than-Nyquist signaling," *IEEE Access*, vol. 9, pp. 86535–86564, 2021, doi: 10.1109/ACCESS.2021.3088997.

[27] J. Fan, S. Guo, X. Zhou, Y. Ren, G. Y. Li, Chen, and Xi, "Faster-than-Nyquist signaling: An overview," *IEEE Access*, vol. 5, pp. 1925–1940, 2017, doi: 10.1109/ACCESS.2017.2657599.

[28] L. B. Y. Du and A. J. Lowery, "Fiber nonlinearity precompensation for long-haul links using direct-detection optical OFDM," *Opt Exp.*, vol. 16, no. 9, pp. 6209–6215, Apr. 2008, doi: 10.1364/OE.16.006209.

[29] G. Tzimpragos, C. Kachris, I. B. Djordjevic, M. Cvijetic, D. Soudris, and I. Tomkos, "A survey on FEC codes for 100 g and beyond optical networks," *IEEE Commun. Surveys Tuts.*, vol. 18, no. 1, pp. 209–221, 1st Quart., 2016, doi: 10.1109/COMST.2014.2361754.

[30] D.-N. Nguyen, J. Bohata, J. Spacil, D. Dousek, M. Komanec, S. Zvanovec, Z. Ghassemlooy, and B. Ortega, "M-QAM transmission over hybrid microwave photonic links at the K-band," *Opt. Exp.*, vol. 27, no. 23, 2019, Art. no. 33745, doi: 10.1364/oe.27.033745.

[31] Quantic PMI. *PS-200M10G-8B-SFF*. Accessed: Jun. 12, 2023. [Online]. Available: https://d2f6h2rm95zg9t.cloudfront.net/81644761/TypicalCharacteristicsonPS-200M10G-8B-SFF-000_ce2684d0-b025-4ed8-bb5c-ce4095046161.pdf
[32] W. Zhu, W. Lv, B. Liao, Y. Zhu, Y. Dai, P. Li, L. Zhang, and Y. Wang, "A 21 to 30-GHz merged digital-controlled high resolution phase shifter-programmable gain amplifier with orthogonal phase and gain control for 5-G phase array application," in *Proc. IEEE Radio Freq. Integr. Circuits Symp. (RFIC)*, Jun. 2019, pp. 67–70, doi: 10.1109/RFIC.2019.8701785.
[33] B. Wang, H. Gao, M. K. Matters-Kammerer, and P. G. M. Baltus, "A 60 GHz 360° phase shifter with 2.7° phase resolution and 1.4° RMS phase error in a 40-nm CMOS technology," in *Proc. IEEE Radio Freq. Integr. Circuits Symp. (RFIC)*, Jun. 2018, pp. 144–147, doi: 10.1109/RFIC.2018.8428980.
[34] S. De, A. Misra, R. Das, T. Kleine-Ostmann, and T. Schneider, "Analysis of non-idealities in the generation of reconfigurable sinc-shaped optical Nyquist pulses," *IEEE Access*, vol. 9, pp. 76286–76295, 2021, doi: 10.1109/ACCESS.2021.3082847.
[35] S. De, K. Singh, C. Kress, R. Das, T. Schwabe, S. PreuBler, T. Kleine-Ostmann, J. C. Scheytt, and T. Schneider, "Roll-off factor analysis of optical Nyquist pulses generated by an on-chip Mach–Zehnder modulator," *IEEE Photon. Technol. Lett.*, vol. 33, no. 21, pp. 1189–1192, Nov. 1, 2021, doi: 10.1109/LPT.2021.3112485.
[36] E. P. da Silva, R. Borkowski, S. Preußler, F. Schwartau, S. Gaiarin, M. I. Olmedo, A. Vedadi, M. Piels, M. Galili, P. Guan, S. Popov, C. Brès, T. Schneider, L. K. Oxenløwe, and D. Zibar, "Combined optical and electrical spectrum shaping for high-baud-rate Nyquist-WDM transceivers," *IEEE Photon. J.*, vol. 8, no. 1, pp. 1–11, Feb. 2016, doi: 10.1109/JPHOT.2016.2523978.
[37] T. Hirooka, P. Ruan, P. Guan, and M. Nakazawa, "Highly dispersion-tolerant 160 Gbaud optical Nyquist pulse TDM transmission over 525 km," *Opt. Exp.*, vol. 20, no. 14, 2012, Art. no. 15001, doi: 10.1364/oe.20.015001.

YOUNUS MANDALAWI received the B.Sc. degree in computer communications engineering from Al-Mansour University College, Baghdad, Iraq, in 2014, and the M.Sc. degree in photonics engineering from Universiti Putra Malaysia, Selangor, Malaysia, in 2019. He is currently pursuing the Ph.D. degree with Institut für Hochfrequenztechnik, Technische Universität Braunschweig, Braunschweig, Germany. His research interests include optical transmission systems and photonics-assisted signal processing.

KARANVEER SINGH (Student Member, IEEE) received the B.S. and M.S. degrees in physical sciences and mathematical sciences from the Indian Institute of Science Education and Research Thiruvananthapuram (IISER-TVM), India, in 2018. He is currently pursuing the Ph.D. degree with Institut für Hochfrequenztechnik, Technische Universität Braunschweig, Germany. His research interests include the designing and characterization of integrated photonic devices and integrated sampling and their application for optical communication.

MOHAMED I. HOSNI received the B.Sc. and M.Sc. degrees in electrical engineering from the Military Technical College (MTC), Cairo, Egypt, in 2009 and 2018, respectively. He is currently pursuing the Ph.D. degree with the Terahertz-Photonics Group, Institut für Hochfrequenztechnik, Technische Universität Braunschweig, Braunschweig, Germany. His research interests include optical communication, frequency comb generation, optical sampling, optical signal processing, and integrated photonics.

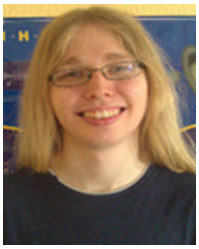

JANOSCH MEIER received the B.Sc. and M.Sc. degrees in physics from the Technical University of Braunschweig, Germany, in 2015 and 2016, respectively. Since 2017, he has been a Research Assistant with the Terahertz-Photonics Group, Institut für Hochfrequenztechnik, Technical University of Braunschweig. His current research interests include optical signal processing, especially photonic digital-to-analog and analog-to-digital conversion.

THOMAS SCHNEIDER received the Diploma degree in electrical engineering from Humboldt Universität zu Berlin, Berlin, Germany, in 1995, and the Ph.D. degree in physics from Brandenburgische Technische Universität Cottbus, Cottbus, Germany, in 2000. From 2000 to 2013, he was with Deutsche Telekom Hochschule für Telekommunikation (HfT), Leipzig, Germany. From 2006 to 2013, he was the Head of Institut für Hochfrequenztechnik, HFT. Since 2014, he has been the Head of the Terahertz-Photonics Group, Institut für Hochfrequenztechnik, Technische Universität Braunschweig, Braunschweig, Germany. His current research interests include nonlinear optical effects in telecommunication systems and sensors, slow and fast light, high-resolution spectroscopy, the generation of millimeter and THz waves, optical sampling, and integrated photonics.